



## Measurement of Electron Density and Temperature of Laser-Induced Copper Plasma

M.A. NAEEM<sup>1,\*</sup>, M. IQBAL<sup>2</sup>, N. AMIN<sup>1</sup>, M. MUSADIQ<sup>1</sup>, Y. JAMIL<sup>1</sup> and F. CECIL<sup>1</sup>

<sup>1</sup>Department of Physics, University of Agriculture, Faisalabad-38040, Pakistan

<sup>2</sup>Department of Chemistry and Biochemistry, University of Agriculture, Faisalabad-38040, Pakistan

\*Corresponding author: E-mail: physicsuaf@yahoo.com

(Received: 5 January 2012;

Accepted: 17 October 2012)

AJC-12311

In present study, the Nd:YAG laser generated copper plasma has been evaluated as a function of distance (0.5-5 mm) at 17.6 and 88.6 mJ. The excitation temperature was determined using Boltzmann plot method of the transitions ( $4p\ P_{3/2} \rightarrow 3d\ 4s\ ^2D_{5/2}$ ) at 510.34 nm ( $4d\ ^2D_{3/2} \rightarrow 4p\ ^2P_{1/2}$ ) at 515.12 nm, ( $4d\ ^2D_{5/2} \rightarrow 4p\ ^2P_{3/2}$ ) at 521.64, whereas electron number density was measured by Stark Broadening method. The spatial behaviour of the electron temperature and electron number density was measured at ambient air pressures. The electron temperature was found in the ranges from 16790-9090 K, while electron number density was  $1.53 \times 10^{17}$ - $1.85 \times 10^{17}$  and  $1.35 \times 10^{17}$ - $1.87 \times 10^{17}\ \text{cm}^{-3}$ , respectively for 17.6 and 88.6 mJ energy. The relationship of electron number density and electron temperature found directly related to laser irradiation, while they were inverse to the distance from the target surface.

**Key Words:** Laser-induced plasma, Plasma spectroscopy, Electron temperature, Electron number density, Laser-induced plasma spectroscopy.

### INTRODUCTION

Due to several key applications in material processing, thin film deposition, environmental monitoring, biomedical studies, military safety usage, art restoration/conservation and metal analysis, the pulsed laser-induced plasmas (LIPs) generated as a result of laser irradiance is of a great interest<sup>1-5</sup>. In this method a highly intense laser pulse interacts with a target material leading to the formation of a micro-plasma in nanosecond due to high intensity plume propagate. The initial part of the plasma is re-heated by the inverse bremsstrahlung (IB) absorption<sup>6-9</sup>. The nature of the laser-induced plasma from a solid target material depends on wavelength, intensity, pulse duration as well as the chemical composition target material and atmospheric conditions such as pressure, space and time<sup>10-15</sup>.

The elemental analysis of the sample based on the optical emission spectra from an laser-induced plasma (LIP) is known as laser-induced plasma spectroscopy (LIPS), also called as laser-induced breakdown spectroscopy (LIBS). The LIBS technique, utilize a pulsed LIP formed near the plasma ignition provide a remote, *in situ*, rapid and multi-elemental analysis of bulk and trace sample in any phase (solid, liquid and gas)<sup>16,17</sup>. For this purpose LIP should be optically thin and under local thermodynamic equilibrium (LTE) condition, the excitation temperature governing the distribution of energy level excitation through the Boltzmann equation and the ionization temperature

governing the ionization equilibrium through the Saha equation should be equal to the electronic temperature describing the Maxwellian distribution of electron velocities. Thus, one describes the plasma in LTE by a common temperature (T), called the plasma temperature. Optical emission spectroscopy has recently attracted a lot of attention for characterization based on LIP. The most widely used spectroscopic method for the determination of T is the Boltzmann plot method which employ the ratio of integrated line intensities for two or more atomic lines. Among several diagnostic methods for measuring the plasma electron density, the plasma spectroscopy based on either Stark broadening of spectral lines or the Saha-Boltzmann equation<sup>4,10</sup>.

The elemental analysis and plasma parameters such as electron number density and electron temperature can be determined from the emission spectrum of the plume<sup>11</sup>. Various researchers world wide have studied and reported the effect of laser irradiation on Cu, Li, Zn, Al, Fe, Pb, Sn, Si and their alloy at different pressures. They also studied the behaviour of electron number density and electron temperature at various laser harmonic level at different distances of target material from the laser irradiance using ranges of spectroscopic methods<sup>8,18,19</sup>.

From last few decades, due to diverse applications as well as ease of utilization, relative simplicity, low cost and highshot-rate capability of laser driven material has become a very

important field and the characterization of material by determining their electron temperature and electron number density is essential for understanding and exploitation of these complex and spectroscopic sources. In the present work, we investigated the Cu plasma produced by the 532 nm of an Nd:YAG laser beam, focused on the Cu target in air. The optical emission was spatially resolved by scanning the plume along path of distribution. We also determined the electron temperature from the relative intensity ratio method and number densities using the Stark line broadening. Further, we have studied the variation of the electron temperature and electron number density with laser irradiance at different distance between target and source.

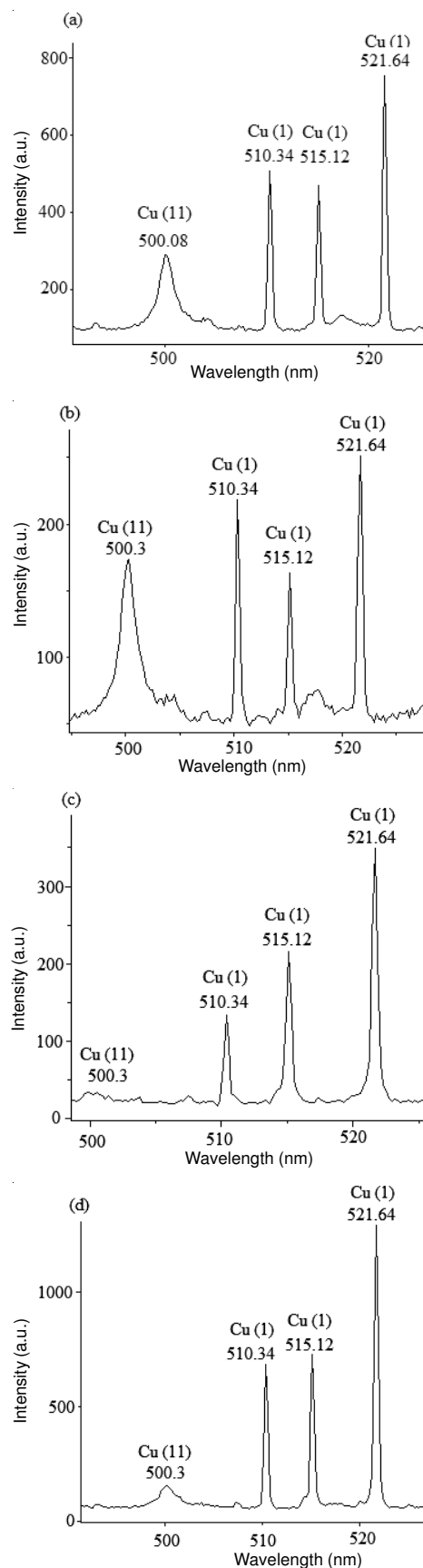
### EXPERIMENTAL

A Q-switched Nd:YAG (Quantel Brilliant) pulsed laser was used for laser beam source, having pulse duration of 5 ns and 10 Hz repetition rate and able to deliver 200 mJ at 532 nm. The laser pulse energy was varied using flash lamp Q-switch delay through laser controller and measured by energy meter. The laser beam was focused on the target using convex lens of 10 cm focal length. The sample was mounted on a 3-dimensional sample stage and rotated to avoid the non-uniform pitting of target material. The distance between the focusing lens and the sample was kept less than the focal length of the lens for the prevention of any breakdown of the ambient air in front of the target. The spectra were recorded by averaging 10 data point of single shot under identical experimental conditions. The radiation emitted from plasma was collected by a fiber optics having a collimating lens (0-45° field of view) placed at right angle to the direction of the laser beam. This optical fiber was connected with HR 2000 detection system (ocean optics) to measure the plasma emission. The data acquired by spectrometers were simultaneously stored on a PC through the HR 2000 software for subsequent analysis<sup>11</sup>.

### RESULTS AND DISCUSSION

The emission spectra of plasma generated at the Cu surface was recorded at different distances along the direction of expansion of the plume at second harmonic 532 nm using energies (17.6 and 88.6 mJ) in ambient air are shown in Figs. 1(a-f), 2(g-l) and 3(m-t). The spectral region can be seen into well separated sections due to either emission from neutral Cu atoms or Cu<sup>2+</sup> ions. From figures it is seen that the Cu(II) is related to the spectral region (495 and 505 nm), while the region of 505-525 nm wavelength is showing the characteristic of Cu(I). We observed a different line form 495-505 nm wavelength indicating the appearance of ions in the excited state. The probability of transitions and identification is given in Table-1. The Cu (II) at lower wavelength belongs to the  $4P^2 P_{3/2} \rightarrow 3d^9 4s^2 \ ^2D_{5/2}$  transition. Fig. 4 depicts the schematic diagram of de-excitation channels liable for the emission lines of the ionized atom. The electron temperature and electron number density trend can easily be observed from well-resolved multiplet structure and a number of excited levels decaying to common lower levels (Figs. 1-3 and 5). The density of the emitted electron was found much high near the surface of the target material which is directly related to the height of spectra recorded from 0.5-5.0 mm distance of target material

(Figs. 1-3). Our observed value of electron temperature and electron number density regarding Cu as function of energy and distance is in accordance with Aragon *et al.*<sup>20</sup>, Hafez *et al.*<sup>21</sup>, Rashid *et al.*<sup>22</sup>, Aragon and Aguilera<sup>19,23</sup>.



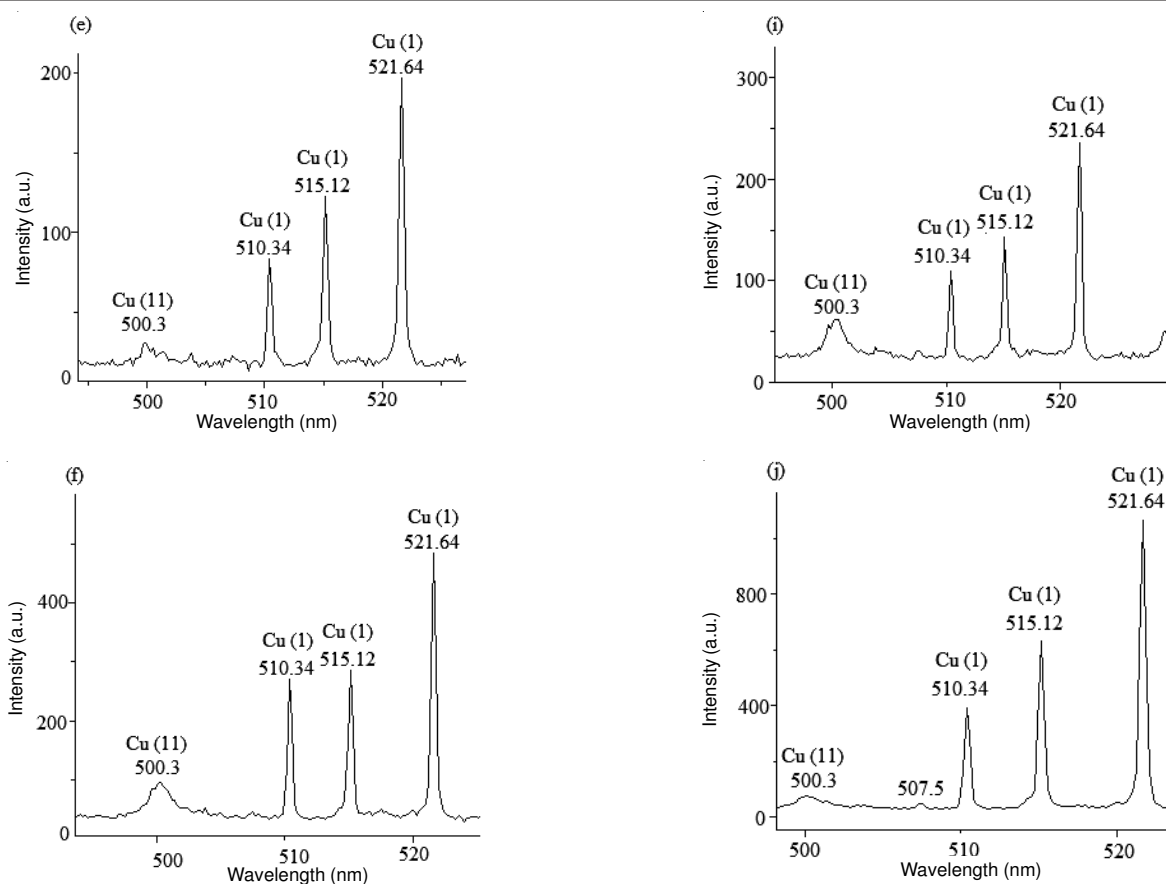


Fig. 1. Emission spectrum generated by the 532 nm laser showing the Cu spectral lines (a) 17.6 mJ at 0.5 mm distance, (b) 88.6 mJ at 0.5 mm, (c) 17.6 mJ at 1 mm, (d) 88.6 mJ at 1 mm, (e) 17.6 mJ at 1.5 mm and (f) 88.6 mJ at 1.5 mm

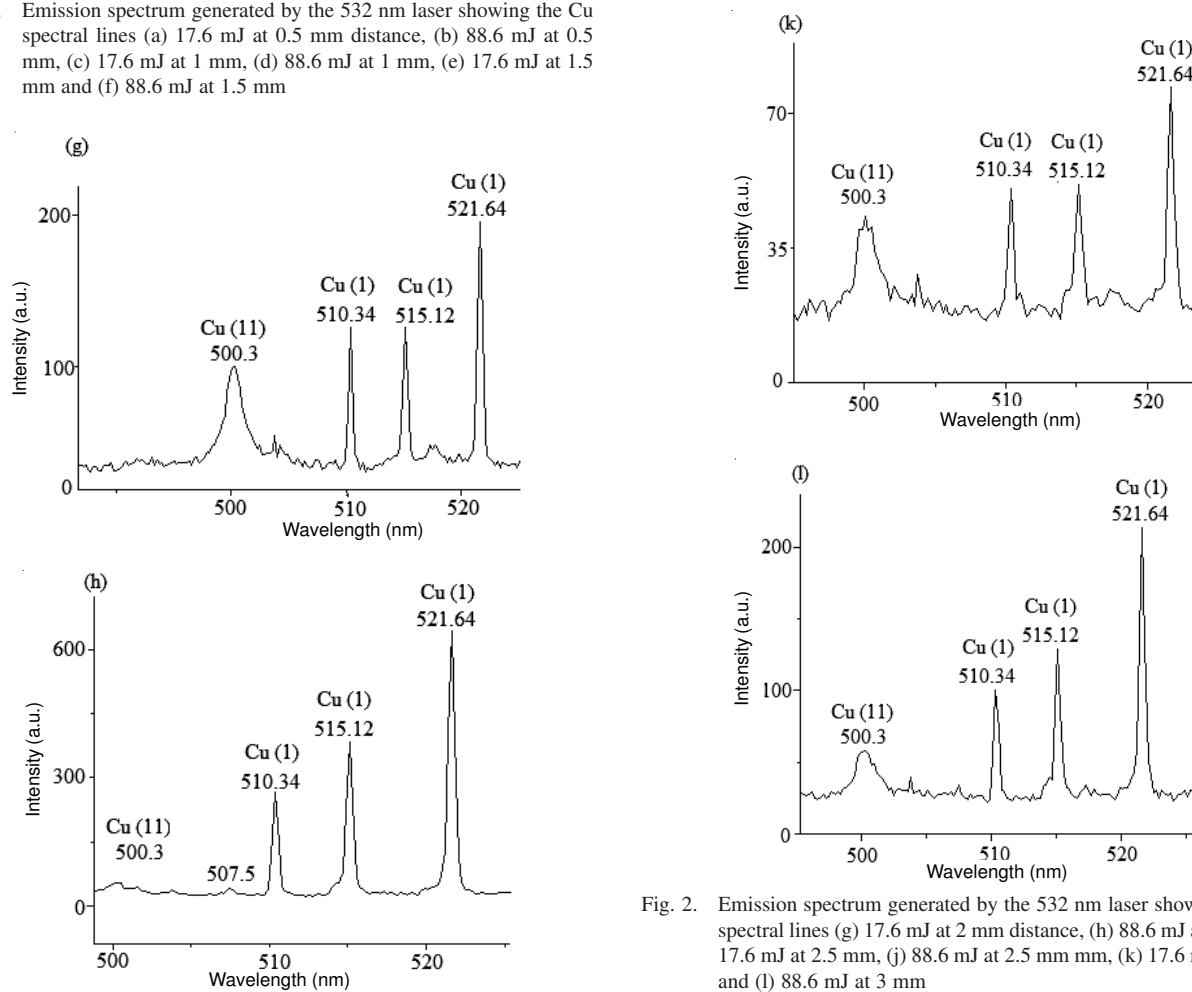


Fig. 2. Emission spectrum generated by the 532 nm laser showing the Cu spectral lines (g) 17.6 mJ at 2 mm distance, (h) 88.6 mJ at 2 mm, (i) 17.6 mJ at 2.5 mm, (j) 88.6 mJ at 2.5 mm mm, (k) 17.6 mJ at 3 mm and (l) 88.6 mJ at 3 mm

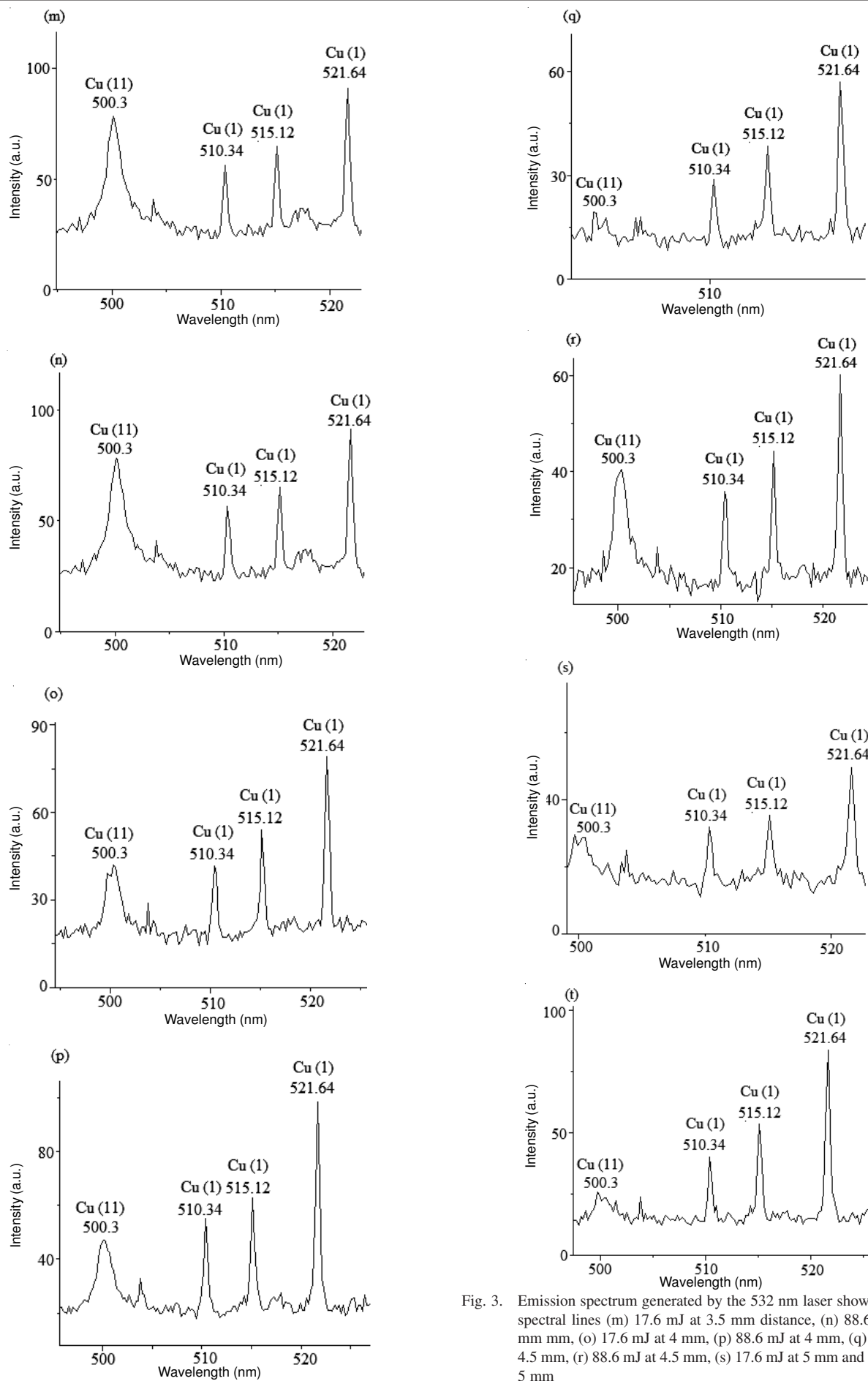


Fig. 3. Emission spectrum generated by the 532 nm laser showing the Cu spectral lines (m) 17.6 mJ at 3.5 mm distance, (n) 88.6 mJ at 3.5 mm mm, (o) 17.6 mJ at 4 mm, (p) 88.6 mJ at 4 mm, (q) 17.6 mJ at 4.5 mm, (r) 88.6 mJ at 4.5 mm, (s) 17.6 mJ at 5 mm and (t) 88.6 mJ 5 mm

**TABLE-1**  
**SPECTROSCOPIC PARAMETERS OF THE OBSERVED SINGLY IONIZED AND NEUTRAL Cu LINES**

Wavelength $\lambda$ (nm)	Transitions	Statistical weight		A ( $s^{-1}$ )	$E_k$ ( $cm^{-1}$ )
		$g_k$	$g_i$		
324.750	$3d4s\ ^2S_{1/2} \rightarrow 3d4p\ ^2P_{3/2}$	4	2	$1.37 \times 10^8$	30783.686
327.395	$3d4s\ ^2S_{1/2} \rightarrow 3d4p\ ^2P_{1/2}$	2	4	$1.36 \times 10^8$	30535.302
464.250	$3d4s5s\ ^2D_{3/2} \rightarrow 3d4s4p\ ^2F_{5/2}$	4	2	$0.074 \times 10^8$	65260.1
510.340	$4p\ ^2P_{3/2} \rightarrow 3d4s\ ^2D_{5/2}$	4	4	$0.020 \times 10^8$	30783.68
515.120	$4d\ ^2D_{3/2} \rightarrow 4p\ ^2P_{1/2}$	4	6	$0.60 \times 10^8$	49935.2
521.640	$4d\ ^2D_{5/2} \rightarrow 4p\ ^2P_{3/2}$	6	2	$0.75 \times 10^8$	49942.057
570.200	$4p\ ^2P_{3/2} \rightarrow 3d4s\ ^2D_{3/2}$	4	4	$0.0028 \times 10^8$	30783.69

$E_k$  = Upper level energy, A = Transition probability.

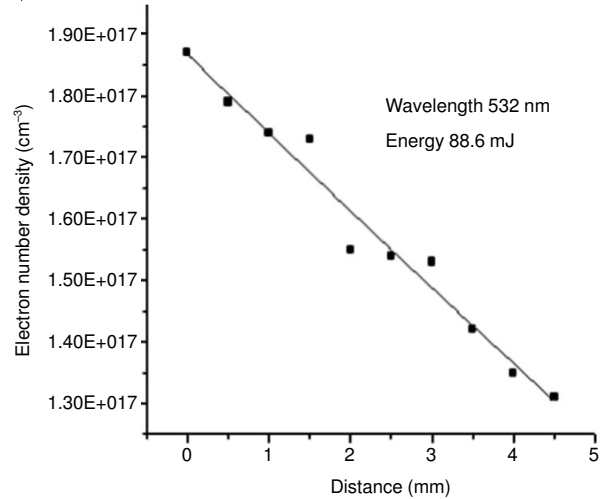
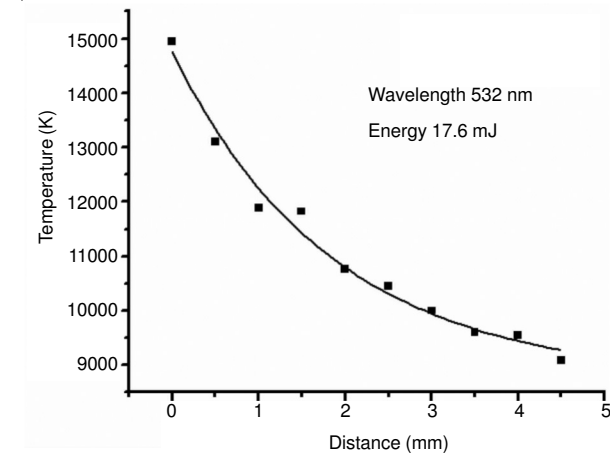


Fig. 4. Effect on electron temperature and electron number density along the direction of propagation of the plume at 532 nm wavelength

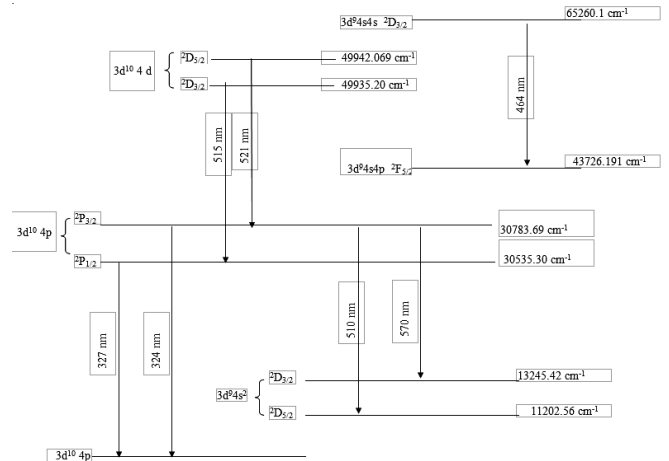
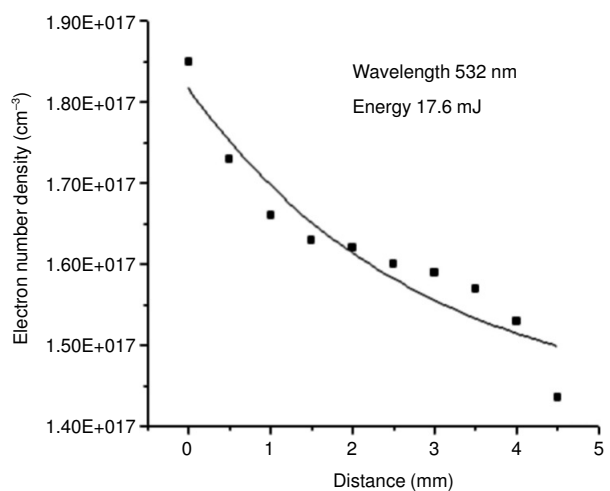
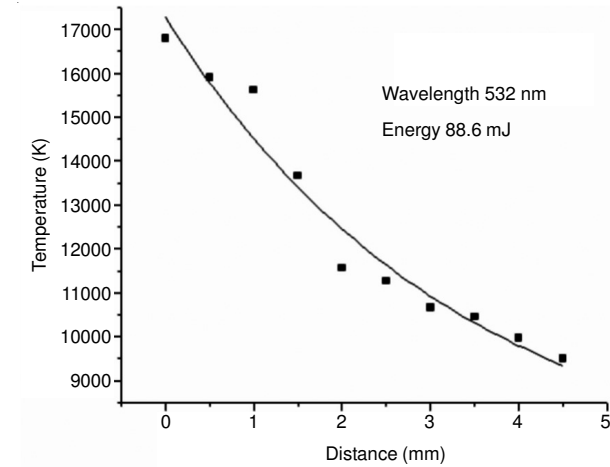


Fig. 5. Energy level diagram of neutral copper showing all the prominent transitions observed in the present experiment

The electron temperature was recorded using the ratio of the relative intensities of spectral lines as described by Shaikh *et al.*<sup>11</sup>.

$$v = \left( \frac{E_i - E_j}{h} \right) \tag{1}$$

$$\frac{dN_{i \rightarrow j}}{dt} = A_{ij}N_i \tag{2}$$

In this equation a unit volume of emitting gas contain  $N_i$  atoms in an excited state of energy  $E_i$  above the ground state and some of them " $dN_{i \rightarrow j}$ " per unit time undergo spontaneous

transitions to lower state of energy " $E_j$ " through emission of an equal number of photons. The number " $dN_{i \rightarrow j}$ " is proportional to the population of the initial state " $N_i$ ".

The emission intensity  $I$  of a line is the energy given out per unit time and is equal to the product of the number  $dN_{i \rightarrow j}$  of produced photons by the energy  $h\nu$  of each photon as:

$$I = A_{ij}h\nu N_i \quad (3)$$

The Boltzmann law states that when thermal equilibrium is attained at absolute temperature ( $T$ ), the average number of particles of a given chemical species  $n_i$  and  $n_j$  with energies  $E_i$  and  $E_j$  can be represented as:

$$\frac{n_i}{n_j} = \exp\left(-\left(\frac{E_i - E_j}{kT}\right)\right) \quad (4)$$

The oldest method for the determination of temperatures in LTE plasma is based on the fact that densities in excited states are proportional to the statistical weight with the exponential of negative ratio of excitation energy and the thermal energy ( $kT$ ), so,

$$N = g \exp\left(-\frac{\Delta E}{kT}\right) \quad (5)$$

where  $g = 2J + 1$  (statistical weight).

$$\frac{I}{gA h\nu} = \exp\left(-\frac{\Delta E}{kT}\right) \quad (6)$$

$$\ln\left(\frac{\lambda I}{gA h c}\right) = -\frac{\Delta E}{kT} \quad (7)$$

$$kT = -\frac{\Delta E}{\ln\left(\frac{\lambda I}{g h c A}\right)} \quad (8)$$

A graph of  $\ln(\lambda I/hcgA)$  versus energy gave a straight line with a slope equal to  $(-1/kT)$ . So, the electron temperature was calculated from the slope as precisely described by Rashid *et al.*<sup>22</sup>. It is well known, the electron temperature and electron number density are dependent to each other and LTE is a condition for the validity of the Boltzmann relationship. In LTE state, it is possible to find a temperature which vary from place to place and follow Boltzmann-Saha distribution as well as the Maxwell distribution regarding electron velocity when the collision is of greater interest than radiative process.

The line identifications and different spectroscopic parameters such as statistical weight ( $g_{(ki)}$ ), transition probability ( $A$ ) wavelength ( $\lambda$ ) and energy ( $E$ ) are given in Table-1, taken from previous reports<sup>22,24,25</sup> and for determination of electron temperature and electron number density, the lines appeared at 510.34, 515.12 and 521.64 nm were used. The electron temperature behaviour was studied as a distance factor from the target surface (0.5-5.0 mm) of the plasma generated by 532 nm wavelength of laser irradiance. The electron temperature near the target surface was found to be very high (16790 K), which was decreased as distance increases (14945 K) form laser source to the Cu target significantly ( $p < 0.01$ ). The electron temperature near Cu surface as well as at 5 mm distance

was found higher for 88.6 mJ versus 17.6 mJ energy. The variation in the electron temperature as a function of distance from the target surface for the plasma produced at 532 nm irradiance (Fig. 4). It is noted that the electron temperature increases with the energy which is surely due to higher energy transfer at this energy level. The region near the surface of the target material constantly absorbs radiation during the exposure time of laser pulse, responsible for enables the electron to gain temperature and so on. According to Rashid *et al.*<sup>22</sup> the higher value of the temperature near the surface is due to the absorption of laser radiation by inverse bremsstrahlung absorption process and decrease in the temperature is due to the fact that the thermal energy is converted rapidly into kinetic energy. The kinetic energy is used to attain maximum expansion velocities and is responsible for decreasing plasma temperature way form the target surface during expansion. Ying *et al.*<sup>26</sup> also reported similar results for ArF excimer laser irradiance in which the temperature varied from 9280-8120 K at a distance ranging from 0-17 mm from the surface of the target.

The minimum electron number density required for the LTE condition was estimated from the relation as precisely described by Lu *et al.*<sup>27</sup>.

$$N_e \geq 1.6 \times 10^{12} T^{1/2} (\Delta E)^3 \quad (9)$$

where  $T$  (K) is the electron temperature and  $\Delta E$  (eV) is the energy difference between the energy states and the electron number density " $N_e$ " was calculated from the width of a spectral line. It is observed that the width of the lines was increased with the increase of laser energy. In plasma, the spectral lines were normally broad and the main sources of the line broadening is doppler broadening and Stark broadening<sup>14</sup>. The Doppler width was estimated from the relation as formula given by Harilal *et al.*<sup>28</sup>.

$$\Delta\lambda = \lambda \sqrt{\frac{8kT \ln 2}{Mc^2}} \quad (10)$$

The Stark broadening line width  $\Delta\lambda_{1/2}$  (FWHM) was calculated using the relation as:

$$\Delta\lambda_{1/2(\text{Stark})} = 2\omega \left(\frac{N_e}{10^{16}}\right) + 3.5A \left(\frac{N_e}{10^{16}}\right)^{1/4} \left[1 - \frac{3}{4} N_D^{-1/3}\right] \omega \left(\frac{N_e}{10^{16}}\right) \quad (11)$$

where " $\omega$ " " $A$ " " $N_e$ " and " $N_D$ " are representing the electron impact width parameter, ion broadening parameter, electron number density and number of particles in the Debye sphere, respectively. The first term refers to the broadening due to the electron contribution, while the second is attributed to the ion broadening. Since the contribution of the ionic broadening is usually very small and neglected. Now, the eqn. 11 reduces to eqn. 12 as:

$$\Delta\lambda_{1/2} = 2\omega \left(\frac{N_e}{10^{16}}\right) \quad (12)$$

The electron number density was determined using the copper line at 510.34 nm emitted observed in the plasma produced by the 532 nm laser irradiance at 17.6 and 88.6 mJ

energy, as can be seen in Fig. 4. In this spatial behaviour of the Cu plasma, the electron number density's were found  $1.53 \times 10^{17}$ - $1.85 \times 10^{17}$  and  $1.35 \times 10^{17}$ - $1.87 \times 10^{17} \text{ cm}^{-3}$ , respectively 17.6 and 88.6 mJ energy level as a function of distance along the direction of plasma expansion. It is evident that the electron number density has a maximum value in the starting region of the plasma and decreased along the direction of expansion constantly. According to Rashid *et al.*<sup>22</sup> the recombination process causes a decrease in the electron number density in the expanded part of the plasma.

It is observed that the electron number density was higher at lower wavelength, indicated that the mass ablation rate would be higher for the shorter wavelength of laser irradiance. Similar relation is also reported by Bogaerts and Chen<sup>29</sup> that mass ablation rate increases as the laser irradiance wavelength is decreased. Similar behaviour of the number density was also reported by Gunther *et al.*<sup>30</sup>. The behaviour of the electron number density and temperature for different values of laser irradiance have been studied in the present work is shown in Fig. 4. It is noted that the electron temperature and electron number density increases with laser irradiance for 88.6 mJ *versus* 17.6 mJ of Nd:YAG laser, but as the distance increased both electron temperature and electron number density decreased constantly. The temperature varies from 9090-16790 K for the 532 nm laser irradiance, whereas the electron number density ranges from  $1.53 \times 10^{17}$ - $1.85 \times 10^{17}$  and  $1.35 \times 10^{17}$ - $1.87 \times 10^{17} \text{ cm}^{-3}$ , respectively for 17.6 and 88.6 mJ. According to Shaikh *et al.*<sup>11</sup> and Rashid *et al.*<sup>22</sup> such behaviour of the electron temperature and electron number density is attributed to the absorption or reflection of the laser energy by plasma and depends on the plasma frequency. They reported lower plasma frequency *versus* laser frequency, which is considered an energy loss in practical applications from the plasma. They also observed more excited species, ions and free electrons as a result of increasing laser irradiance. The laser pulse interacts with these species and resulted further heating and ionization and consumption of the incoming laser energy. The plasma absorption energy by inverse bremsstrahlung absorption (IB) and photoionization. Rashid *et al.*<sup>22</sup>, Shaikh *et al.*<sup>11</sup> calculated the inverse bremsstrahlung process and showed that the inverse bremsstrahlung process is more efficient in the case of infrared and visible than the ultraviolet (UV) due to the  $\lambda^3$  dependence of the electron-ion inverse bremsstrahlung process. Similar results has also been reported by various other researcher<sup>4,16-18,20,21</sup> regarding the electron number density behaviour as a function of energy and distance for different metals.

### Conclusion

The effect of Q-switched Nd:YAG laser on Cu plasma generation by the second harmonics on electron temperature, electron number density and their behaviour as a function of distance along the direction of expansion of the plasma. The results reveal that both electron temperature and electron

number density decreases along the direction of propagation of the plasma. Furthermore, the relationship of electron number density and electron temperature is directly related to laser irradiance and inverse of the distance from the target surface.

### ACKNOWLEDGEMENTS

The authors are thankful Dr. Nek Muhammad Shaikh, Quaid e Azam University, Islamabad, for technical assistance during the research work.

### REFERENCES

1. M. Tang, V. Shim, Z.Y. Pan, Y.S. Choo and M.H. Hong, *J. Laser Micro/Nanoeng.*, **6**, 6 (2011).
2. S.B. Mansour and B.S. Yilbas, *Curr. Appl. Phys.*, **10**, 1243 (2010).
3. S.M. Pawar, A.V. Moholkar, I.K. Kim, S.W. Shin, J.H. Moon, J.I. Rhee and J.H. Kim, *Curr. Appl. Phys.*, **10**, 565 (2010).
4. V.K. Unnikrishnan, K. Alti, V.B. Kartha, C. Santhosh, G.P. Gupta and B.M. Suri, *Pramana J. Phys.*, **74**, 983 (2010).
5. C.-Y. Ho, Y.-H. Tsai, C.-S. Chen and M.-Y. Wen, *Curr. Appl. Phys.*, **11**, S301 (2011).
6. P. Stavropoulos, C. Palagas, G.N. Angelopoulos, D.N. Papamantellos and S. Couris, *Spectrochim. Acta B*, **59**, 1885 (2004).
7. J.L.H. Chau, C.-Y. Chen, M.-C. Yang, K.-L. Lin, S. Sato, T. Nakamura, C.-C. Yang and C.-W. Cheng, *Mater. Lett.*, **65**, 804 (2011).
8. K.A. Bhatti, M. Khaleeq-ur-Rahman, M.S. Rafique, K.T. Chaudhary and A. Latif, *Vacuum*, **84**, 980 (2010).
9. E.D. Ali, H.A. Vural, B. Ortaç and T. Uyar, *Mater. Lett.*, **65**, 2941 (2011).
10. H.R. Griem, *Principles of Plasma Spectroscopy*, Cambridge Uni. Press, Cambridge (1997).
11. N.M. Shaikh, B. Rashid, S. Hafeez, Y. Jamil and M.A. Baig, *J. Phys. D Appl. Phys.*, **39**, 1384 (2006).
12. M. Wolter, M. Hundt and H. Kersten, *Vacuum*, **85**, 482 (2010).
13. K.A. Bhatti, M.S. Rafique, M. Khaleeq-ur-Rahman, A. Latif, K. Hussain, A. Hussain, K.T. Chaudhary, B.A. Tahir and R. Qindeel, *Vacuum*, **85**, 915 (2011).
14. K.A. Bhatti, M. Khaleeq-ur-Rahman, H. Jamil, A. Latif and M.S. Rafique, *Vacuum*, **84**, 1080 (2010).
15. R.T. Rumianowski and R.S. Dygdala, *Vacuum*, **76**, 501 (2004).
16. A.W. Miziolek, V. Pallesschi and I. Schecchter, *Laser-Induced Breakdown Spectroscopy*, Cambridge University Press, Cambridge (2006).
17. D.A. Cremers and L.J. Radziemski, *Handbook of Laser-Induced Breakdown Spectroscopy*, John Wiley & Sons Ltd., West Sussex (2006).
18. G. Abdellatif and H. Imam, *Spectrochim. Acta B*, **57**, 1155 (2002).
19. C. Aragón and J.A. Aguilera, *Spectrochim. Acta B*, **65**, 395 (2010).
20. C. Aragon, J. Bengoechea and J.A. Aguilera, *Spectrochim. Acta B*, **56**, 619 (2001).
21. M.A. Hafez, M.A. Khedr, F.F. Elaksher and Y.E. Gamal, *Plasma Source Sci. Technol.*, **12**, 185 (2003).
22. B. Rashid, S. Hafeez, N.M. Shaikh, M. Saleem, R. Ali and M.A. Baig, *Int. J. Modern Phys. B*, **121**, 2697 (2007).
23. C. Aragón and J.A. Aguilera, *Spectrochim. Acta B*, **63**, 893 (2008).
24. K. Fu, M. Jogvich, M. Knebel and K. Wiesemann, *Atomic Data Nucl. Data Tables*, **61** (1995).
25. C.E. Moore, *Atomic Energy Levels*, NBS Circular No. 467, Washington DC (1971).
26. M. Ying, Y. Xia, Y. Sun, M. Zhao, Y. Ma, X. Liu, Y. Li and X. Hou, *Laser Particle Beams*, **21**, 97 (2003).
27. Y. Lu, Z. Tao and M. Hong, *J. Jpn. Appl. Phys.*, **38**, 2958 (1999).
28. S.S. Harilal, B. O'Shay, M.S. Tillack and M.V. Mathew, *J. Appl. Phys.*, **98**, 1 (2005).
29. A. Bogaerts and Z. Chen, *Spectrochim. Acta B*, **60**, 1280 (2005).
30. D. Gunther, S.E. Jackson and H.P. Longrich, *Spectrochim. Acta B*, **54**, 381 (1999).